Am J Nucl Med Mol Imaging 2013;3(1):85-96
www.ajnmmi.us /ISSN:2160-8407/ajnmmi1210001

Original Article

Characterization of primary prostate carcinoma by *anti*-1-amino-2-[^{18}F] -fluorocyclobutane-1-carboxylic acid (*anti*-3-[^{18}F] FACBC) uptake

David M Schuster[1], Pooneh A Taleghani[1], Peter T Nieh[2], Viraj A Master[2], Rianot Amzat[1], Bital Savir-Baruch[1], Raghuveer K Halkar[1], Tim Fox[3], Adeboye O Osunkoya[2,4], Carlos S Moreno[4], Jonathon A Nye[1], Weiping Yu[1], Baowei Fei[1], Zhibo Wang[5], Zhengjia Chen[5], Mark M Goodman[1]

[1]*Department of Radiology and Imaging Sciences, Emory University;* [2]*Department of Urology, Emory University;* [3]*Department of Radiation Oncology, Emory University;* [4]*Pathology and Laboratory Medicine, Emory University;* [5]*Department of Biostatistics and Bioinformatics, Emory University, Atlanta, GA, USA*

Received October 7, 2012; Accepted December 10, 2012; Epub January 5, 2013; Published January 15, 2013

Abstract: Anti-1-amino-3-[^{18}F] fluorocyclobutane-1-carboxylic acid (*anti*-3-[^{18}F] FACBC) is a synthetic amino acid positron emission tomography (PET) radiotracer with utility in the detection of recurrent prostate carcinoma. The aim of this study is to correlate uptake of *anti*-3-[^{18}F] FACBC with histology of prostatectomy specimens in patients undergoing radical prostatectomy and to determine if uptake correlates to markers of tumor aggressiveness such as Gleason score. Ten patients with prostate carcinoma pre-radical prostatectomy underwent 45 minute dynamic PET-CT of the pelvis after IV injection of 347.8 ± 81.4 MBq *anti*-3-[^{18}F] FACBC. Each prostate was co-registered to a separately acquired MR, divided into 12 sextants, and analyzed visually for abnormal focal uptake at 4, 16, 28, and 40 min post-injection by a single reader blinded to histology. SUVmax per sextant and total sextant activity (TSA) was also calculated. Histology and Gleason scores were similarly recorded by a urologic pathologist blinded to imaging. Imaging and histologic analysis were then compared. In addition, 3 representative sextants from each prostate were chosen based on highest, lowest and median SUVmax for immunohistochemical (IHC) analysis of Ki67, synaptophysin, P504s, chromogranin A, P53, androgen receptor, and prostein. 79 sextants had malignancy and 41 were benign. Highest combined sensitivity and specificity was at 28 min by visual analysis; 81.3% and 50.0% respectively. SUVmax was significantly higher ($p<0.05$) for malignant sextants (5.1±2.6 at 4 min; 4.5±1.6 at 16 min; 4.0±1.3 at 28 min; 3.8±1.0 at 40 min) compared to non-malignant sextants (4.0±1.9 at 4 min; 3.5±0.8 at 16 min; 3.4±0.9 at 28 min; 3.3±0.9 at 40 min), though there was overlap of activity between malignant and non-malignant sextants. SUVmax also significantly correlated ($p<0.05$) with Gleason score at all time points ($r=0.28$ at 4 min; $r=0.42$ at 16 min; $r=0.46$ at 28 min; $r=0.48$ at 40 min). There was no significant correlation of *anti*-3-[^{18}F] FACBC SUVmax with Ki-67 or other IHC markers. Since there was no distinct separation between malignant and non-malignant sextants or between Gleason score levels, we believe that *anti*-3-[^{18}F] FACBC PET should not be used alone for radiation therapy planning but may be useful to guide biopsy to the most aggressive lesion.

Keywords: Positron emission tomography (PET), prostate carcinoma, *anti*-3-[^{18}F] FACBC

Introduction

Prostate carcinoma is the second leading cause of death in men in the United States. It is estimated that 241,740 new cases of prostate cancer will be diagnosed in 2012, leading to 28,170 prostate cancer-related deaths [1]. Yet, the rate of tumor growth of primary prostate carcinoma is very heterogenous. While the highly aggressive phenotype may rapidly metastasize leading to death, many other cases of prostate cancer are asymptomatic or are never detected with subsequent death from unrelated causes [2]. Upon serum PSA elevation, transrectal guided ultrasound with biopsy is typically employed as a next step, yet is invasive and subject to sampling error [3-5].

While magnetic resonance imaging (MR) is currently the most valuable widely available imaging modality in the characterization of primary prostate carcinoma, it suffers from limitations,

especially in the post-biopsy setting, including the ability to differentiate benign from malignant tissue and the lack of routinely accessible metabolic data [6]. Thus, there is no universally accepted method, imaging or biomarker available that can be used to decide which tumor will require aggressive therapy and which can be followed with active surveillance. Yet the availability of such imaging biomarkers would be useful to not only stratify patients into therapeutic categories, but also to more accurately direct biopsy, and to define tumor volumes for intensity modulated radiotherapy (IMRT) and other advanced techniques [7].

Anti-1-amino-3-fluorine 18 –fluorocyclobutane-1-carboxylic acid (*anti*-3-[^{18}F] FACBC) is a synthetic amino acid analog positron emission tomography (PET) radiotracer that has demonstrated promise for the staging and restaging of prostate carcinoma [8, 9]. The uptake of *anti*-3-[^{18}F] FACBC is likely mediated via sodium-dependent (ASC) and sodium-independent (L type) amino acid transporters (AATs). *Anti*-3-[^{18}F] FACBC is not metabolized nor highly excreted in urine [10-12]. The purpose of this study is to determine if uptake of *anti*-3-[^{18}F] FACBC in pre-surgical prostatectomy patients with known prostate carcinoma correlates with the presence or absence of neoplasia on a sextant analysis and if the degree of radiotracer uptake correlates with markers of tumor aggressiveness such as Gleason score.

Materials and methods

Preparation of anti-3-[^{18}F] FACBC

The preparation of *anti*-3-[^{18}F] FACBC has been previously reported [13]. The decay-corrected radiochemical yield of the desired product was 24%, and its radiochemical purity was 99% 80 minutes after the end of bombardment. The mass of amino acids, predominantly *anti* -1-amino-3- hydroxy cyclobutane-1-carboxylic acid, in the production batch was approximately 1.5 mg or 9.0 μmol. The specific activity of *anti*-3-[^{18}F] FACBC was determined to be 580–820 MBq/μmol based on *the quantity of anti* -1-amino-3-hydroxycyclobutane-1-carboxylic acid present in the *anti*-3-[^{18}F] FACBC batch production at the end of synthesis.

Patient selection

This prospective study was approved by the institutional review board and complied with Health Insurance Portability and Accountability Act guidelines, and conducted under the auspices of IND 72437 from the United States Food and Drug Administration. Written informed consent was obtained. Patients were enrolled in this study if the following criteria were met: a) 18 years of age or older; b) scheduled for prostatectomy based on a diagnosis of primary prostate cancer; c) ability to lie still for PET scanning; d) able to provide written informed consent.

Anti-3-[^{18}F] FACBC imaging protocol

Scanning was conducted by using a PET/CT unit (Discovery DLS; GE Medical Systems, Milwaukee, WI). All patients fasted for 4–6 hours before undergoing scanning with *anti*-3-[^{18}F] FACBC. Subjects first underwent CT of the pelvis (80–120 mA, 120 kVp) with oral contrast and without intravenous contrast. 347.8 ± 81.4 MBq of *anti*-3-[^{18}F] FACBC (161.7 - 469.9 MBq) was injected intravenously over 2 minutes. Dynamic PET at the level of the prostate was then performed for 17 individual frames at a dynamic frame rate of 2x15 sec, 5x30 sec, 5x60 sec, and 9x4 min (frames x time-per-frame). The entire study including injection of radiotracer lasted approximately 43 minutes. PET images were reconstructed with iterative technique (2 iterations, 28 subsets) and registered to the CT using standard techniques.

MRI imaging protocol

Routine pre-surgical prostatectomy pelvic MR was performed on a 1.5 T MR scanner with a body surface coil (Avanto; Siemens Medical Systems, Malvern, PA) using a combination of high resolution T1 and T2, dynamic 3D gradient echo perfusion with gadolinium contrast enhancement, and three-dimensional breath-held spoiled gradient echo with fat saturation. Only the T2 weighted studies were used for co-registration to the *anti*-3-[^{18}F] FACBC PET-CT. In detail, the T2 imaging was performed using an interleaved fast spin echo imaging (TSE) sequence, which covered 30 x 4 mm slices (0.8mm gap). The field-of-view was 200x200mm (with fold-over suppression), with a 256x230 matrix (interpolated to 512), enabling an in-plane resolution of 0.4x0.5mm. The TR/TE was 3000/95ms, using a turbo factor of 13 with linear k-space ordering (bandwidth = 130Hz/px). The subject was allowed to breathe freely; how-

ever, three signal averages and anterior saturation bands were implemented to lessen respiration artifacts.

Image processing

The PET-CT images and the T2 weighted MR images were then imported into an institutional image registration platform (Velocity; Velocity Medical Solutions, Atlanta, GA) for automatically creating a rigid transformation (rotation and translations) between the MR and CT images. The rigid registration algorithm considers simultaneously rotations and translations on all axes and allows definition of a volume of interest (VOI) to focus the registration on the prostate anatomy only. For this particular analysis we selected the Mattes formulation of the mutual information as it is better suited to deal with differences in Hounsfield units (HU) calibration as compared to single-modality metrics such as mean squares [14]. The use of a VOI is essential for the automated registration, as it allows the algorithm to consider only voxels within the vicinity of the prostate volume. Subjective physician review of the image registration from this automated method confirmed ideal superimposition of the two datasets within the VOI.

The rigid transformation from the MR-CT registration was then applied to the PET image study with the PET imaging data corresponding to the MR's spatial coordinate system. Minor adjustments were then made to best register and fine tune the PET to the MR prostate data registration since different degrees of bladder filling may result in shifting of pelvic contents between the two studies. The resultant registered PET-MR image was then resampled into the same DICOM frame of reference coordinate space to be exported as a DICOM object into a dedicated reading workstation (MIMvista 4.2-5.2; MIMvista, Cleveland, OH). Since the prostate lies in the pelvis typically at an anteriorly tilted angle, and the pathologic specimen is processed at our institution with a freehand approach and sliced perpendicular to the plane of the urethra, the fused sagittal image was tilted obliquely to best match the angle at which histologic processing occurred. Resliced angles were typically 20-40 degrees from original orientation.

At this point, the margins of the prostate were defined on the MR and a point midway between the superior and inferior borders of the gland was chosen and marked as "mid-gland". At points midway between the inferior and superior borders and the mid-gland, apex and base levels were similarly identified and marked. In this manner, we were best able to match imaging to histologic processing. Each of the 3 levels were then divided into sextants (right/left and anterior/posterior at apex, mid and base) with a freehand drawing tools provided in the software package and saved as part of the PET-MR dataset.

Image analysis

All *anti*-3-[^{18}F] FACBC PT-MR images were interpreted visually by a board certified nuclear radiologist (DMS) blinded to the histologic results. A region in the prostate was considered positive if there were asymmetric focal activity exceeding prostate background activity similar to the criteria utilized by Yamaguchi in studying ^{11}C-Choline PET of the prostate [15]. Each of 12 sextants per prostate were analyzed separately at 4, 16, 28 and 40 min post-injection for the presence or absence of focal activity suspicious for tumor. SUVmax, SUVmean, and total sextant activity (TSA) of each sextant was also calculated (SUV*ml) using the entire anatomic volume of the sextant in that imaging plane. SUV mean of representative background of the prostate as well as other structures such as blood pool at the iliac vessels, marrow at the ilium, and muscle in the gluteus were also recorded.

Pathology protocol

Following *anti*-3-[^{18}F] FACBC scanning, all candidates underwent radical prostatectomy. All pathologic samples underwent standard histologic analysis to determine where prostate carcinoma glands were present. Specimens were sectioned perpendicular to the urethra using a freehand method at 4mm thickness and quadrisected. Tissues were submitted in histology cassettes with the original section and anatomical quadrant clearly identified and labeled. The tissue were then fixed in 10% neutral-buffered formalin, embedded in wax, and stained with hematoxylin & eosin (H&E) using standard histologic techniques. Each tissue slide was evaluated for involvement by carcinoma, prostatic intraepithelial neoplasia, prostatic hypertrophy and inflammation. The presence or absence of

tumor in each quadrant and Gleason scores when applicable were recorded by a board certified Urologic Pathologist (AOO) blinded to imaging results.

Correlation of imaging to histologic data

The presence or absence of tumor on a sextant basis predicted by *anti*-3-[^{18}F] FACBC PET images was correlated to the similar histopathologic analysis. Diagnostic performance was thus calculated. Mean (+/- SD) uptake parameters such as SUVmax of each sextant were calculated for malignant and non-malignant sextants. Similarly for the malignant sextants, radiotracer uptake was correlated with Gleason score. In a preliminary analysis we noted that all specimens except one had varying degrees of benign prostatic hypertrophy (BPH) involving all sextants. Because of our inability to effectively model the exact location of histology to imaging in all but a few instances, we believed that we could not accurately conduct a subanalysis of normal tissue versus BPH, prostatic intraepithelial neoplasia (PIN) or inflammation. Thus, we confined our analysis to presence or absence of malignancy at the sextant level only.

Immunohistochemical analysis

Three representative sextants believed to be malignant were chosen based on highest, lowest and median SUVmax from each prostate for immunohistochemical (IHC) analysis of the Ki-67 proliferation index. Five micron sections of formalin-fixed, deparaffinized tissue from each case was immunostained using antibodies against Ki-67 (clone MIB1, 1:160 dilution, DAKO Corp, Carpinteria, CA) using tonsil as the positive control. Negative controls were run simultaneously and had primary antibody replaced with buffer. Antigen retrieval was conducted in citrate buffer at pH 6.0 under a pressure of 15 pounds per square inch for 3 minutes. Envision+ Dual Link Kit (DAKO Corp) was used as the detection system, with diaminobenzidine as the chromogen and hematoxylin as the counterstain. Staining was performed with the DAKO Autostainer. Expression of Ki-67 in the malignant lesions was then correlated with *anti*-3-[^{18}F] FACBC uptake. Similar processing was applied for the other IHC indices of synaptophysin, P504s, chromogranin A, P53, androgen receptor, and prostein.

Statistical analysis

Descriptive statistics were used to summarize the data with mean and standard deviation (SD) for each outcome variable among each of the groups. The sensitivity, specificity, PPV, NPV, and accuracy were estimated as proportion and their 95% CI were constructed assuming a binomial distribution. Two samples T-test was employed to compare the differences between malignant and non-malignant sextants. Pearson/Spearman correlation coefficients were estimated to measure the relationship between SUVmax of *anti*-3-[^{18}F] FACBC uptake and each of other covariates and tested using Wald's test. Two sample t-test was also used to test the SUVmax of *anti*-3-[^{18}F] FACBC uptake between two groups stratified by Gleason score (3+4 or less vs 4+3 or greater). Linear regression analysis was performed on association of SUV max with optical IHC signal and the radiotracer retention index as well as other factors among early and delayed imaging, respectively. Plots were also generated to depict the relationships of each pairwise variables graphically. The significance level was set at 0.05 for all tests. The SAS statistical package V9.2 (SAS Institute, Inc., Cary, NC) was used for data managements and analyses.

Results

Demographics

Ten patients were studied between March 10, 2009, and April 21, 2012. No adverse events were reported. Mean age was 60.8 years ± 6.3 (range, 49-70 y) and the mean PSA level was 8.2ng/mL ± 5.3 (range, 2.3-16.6). 3 patients had a PSA level of less than 4 ng/mL, three patients had a level between 4 and 10 ng/mL, and four had a level greater than 10 ng/mL. One hundred twenty sextants were analyzed in 10 patients: 79 malignant and 41 non-malignant. Gleason score of the tumor lesions varied between 3+3=6 and 5+5=10. 21 sextants contained tumor with a Gleason score of 3+3=6, 17 with 3+4=7, 9 with 4+3=7, 20 with 4+4=8 and 12 with 5+5=10.

Anti-3-[^{18}F] FACBC PET/CT diagnostic performance

Correlation of imaging positivity per sextant as compared with blinded histopathologic analy-

Table 1. Diagnostic performance per sextant at each time point by visual analysis

	4mins	16mins	28mins	40mins
True positive	71	68	65	63
True negative	7	14	20	15
False positive	32	25	20	25
False negative	8	13	15	17
Total	118	120	120	120
Sensitivity (CI)%	89.9 (80.5-95.2)	84.0 (73.8-90.9)	81.3 (70.6-88.8)	78.8 (67.9-86.8)
Specificity (CI)%	18.0 (8.1-34.11)	35.9 (21.7-52.9)	50.0 (34.1-65.9)	37.5 (23.2-54.2)
PPV (CI)%	68.9 (59.0-77.5)	73.1 (62.8-81.5)	76.5 (65.8-84.7)	71.6 (60.8-80.5)
NPV (CI)%	46.7 (22.3-72.6)	51.9 (32.4-70.9)	57.1 (39.5-73.2)	46.9 (29.5-65.0)
Accuracy (CI)%	66.1 (56.7-74.4)	68.3 (59.1-76.4)	70.8 (61.7-78.6)	65.0 (55.7-73.3)

sis of the sextants at time points is presented in **Table 1** along with diagnostic performance and confidence intervals. Because of a technical error, 2 of 120 sextants from the 4 minute time point could not be analyzed. Highest combined diagnostic performance for *anti*-3-[^{18}F] FACBC was at 28 min with 65 true positive tumor sextants, 20 true negative sextants, 20 false positive sextants, and 15 false negative sextants. Sensitivity, specificity, and accuracy were 81.3%, 50.0%, 70.8% respectively, with a positive predictive and negative predictive value of 76.5% and 57.1% respectively. **Figure 1** and **2** are representative correlative images with histology.

Anti-3-[^{18}F] FACBC PET quantitative analysis compared with presence or absence of tumor

Sextant SUV max and total sextant activity was significantly higher for malignant sextants compared to non-malignant sextants at all time points as presented in **Table 2A** and **2B**. Though the differences of mean values were statistically significant, overlap of SUVmax and TSA activity between malignant and non-malignant sextants was present.

Correlation of malignant sextant SUVmax with Gleason score

For the 79 malignant sextants there was significant correlation of SUVmax and Gleason score at all time points (r=0.28 at 4 min; r=0.42 at 16 min; r=0.46 at 28 min; r=0.48 at 40 min) as presented in **Figure 3**. In addition, when grouping Gleason score as 3+4 or less and 4+3 or greater there is a statistically significant difference of mean SUVmax at all time points as illustrated in **Table 3**. Though the differences were statistically significant, overlap of mean SUVmax limits between Gleason scores was present. Note that there were no sextants with Gleason 4+5 or 5+4.

Correlation of SUVmax and PSA per patient

When SUVmax of each prostate was correlated with the PSA of each of the patients at time of surgery, a positive trend was noted at each time point (r=0.53 at 4 min; r=0.59 at 16 min; r=0.37 at 28 min; r=0.45 at 40 min) but which did not reach statistical significance (p>0.05).

Immunohistochemical analysis including Ki67

30 sextants (3 sextants from each extant prostate) were chosen for analysis per above criteria. Out of the 30 chosen sextants, 18 malignant sextants could be analyzed. 12 were technically inadequate. SUV max of malignant samples had no significant correlation (p>0.05) with Ki-67 (r=-0.10 at 4 min; r=0.01 at 16 min; r=0.24 at 28 min; r=0.11 at 40 min), synaptophysin (r=0.25 at 4 min; r=0.23 at 16 min; r=0.24 at 28 min; r=0.14 at 40 min), P504s (r=-0.02 at 4 min; r=-0.18 at 16 min; r=-0.22 at 28 min; r=-0.15 at 40 min), chromogranin A (r=-0.04 at 4 min; r=0.17 at 16 min; r=0.11 at 28 min; r=0.15 at 40 min), P53 (r=-0.40 at 4 min;

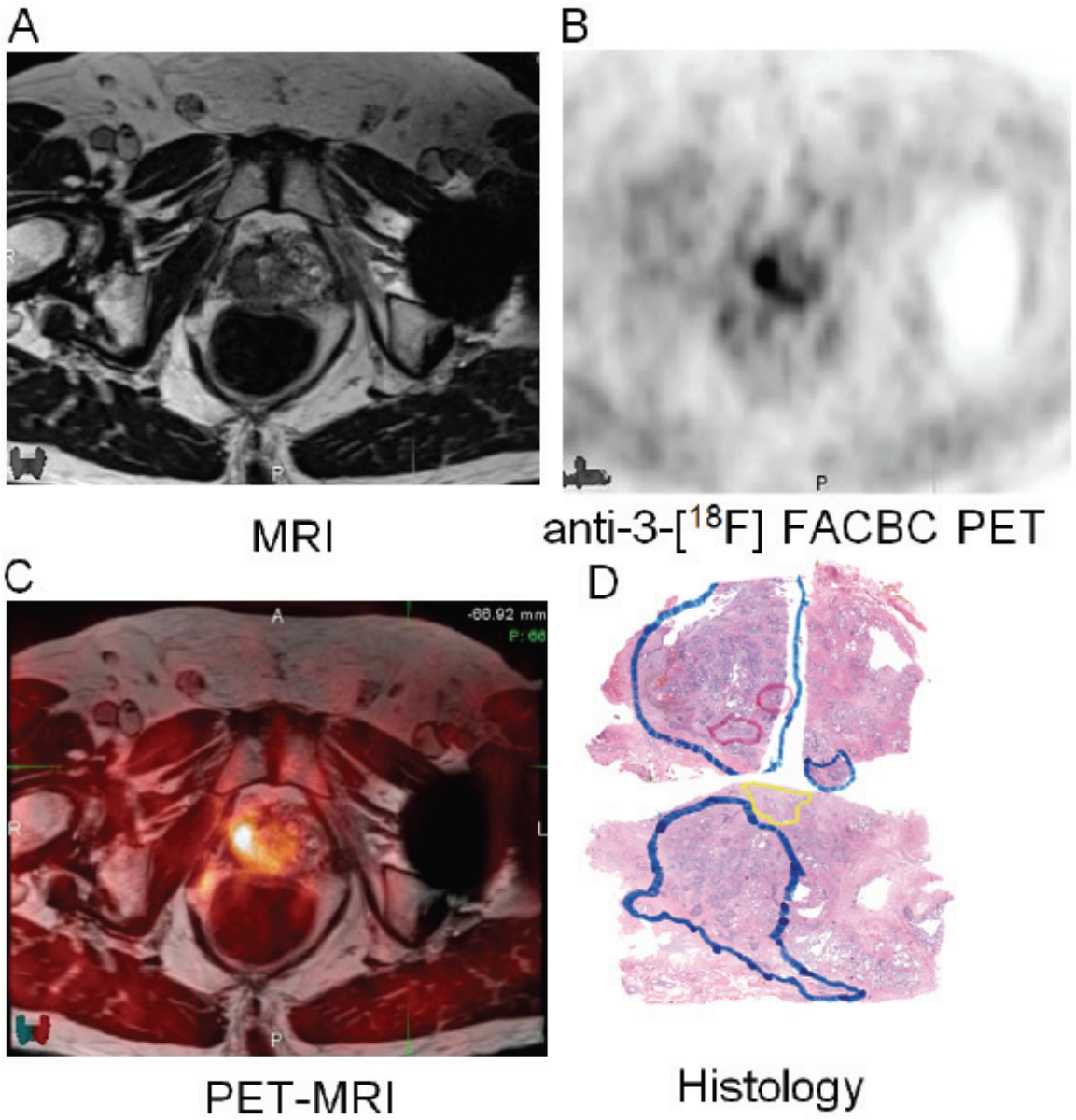

Figure 1. MR (A), *anti*-3-[^{18}F] FACBC PET acquired at 28 min post radiotracer administration (B), coregistered PET-MR (C) and histology (D). In this patient uptake in the right anterior and posterior mid sextants correlate with presence of tumor while a small tumor focus in the left anterior sextant is not visualized. On the histology, solid blue represent Gleason 4, solid red represents Gleason 5, and yellow represents BPH.

r=-0.22 at 16 min; r=0.03 at 28 min; r=-0.05 at 40 min), androgen receptor (r=-0.39 at 4 min; r=-0.38 at 16 min; r=-0.40 at 28 min; r=-0.26 at 40 min), or prostein (r=0.28 at 4 min; r=0.29 at 16 min; r=0.06 at 28 min; r=-0.03 at 40 min).

Discussion

We set out to determine if *anti*-3-[^{18}F] FACBC PET uptake in primary prostate carcinoma correlated with presence or absence of tumor and if the degree of uptake corresponded to biomarkers of tumor aggressiveness such as Gleason Score and Ki-67. We found that based upon blinded sextant visual analysis, highest diagnostic performance occurred at 28 minutes post-injection with a sensitivity of 81.3% but a specificity of 50.0%. Statistically significant differences between mean SUVmax and total sextant activity between malignant and non-malignant sextants were noted, as well as

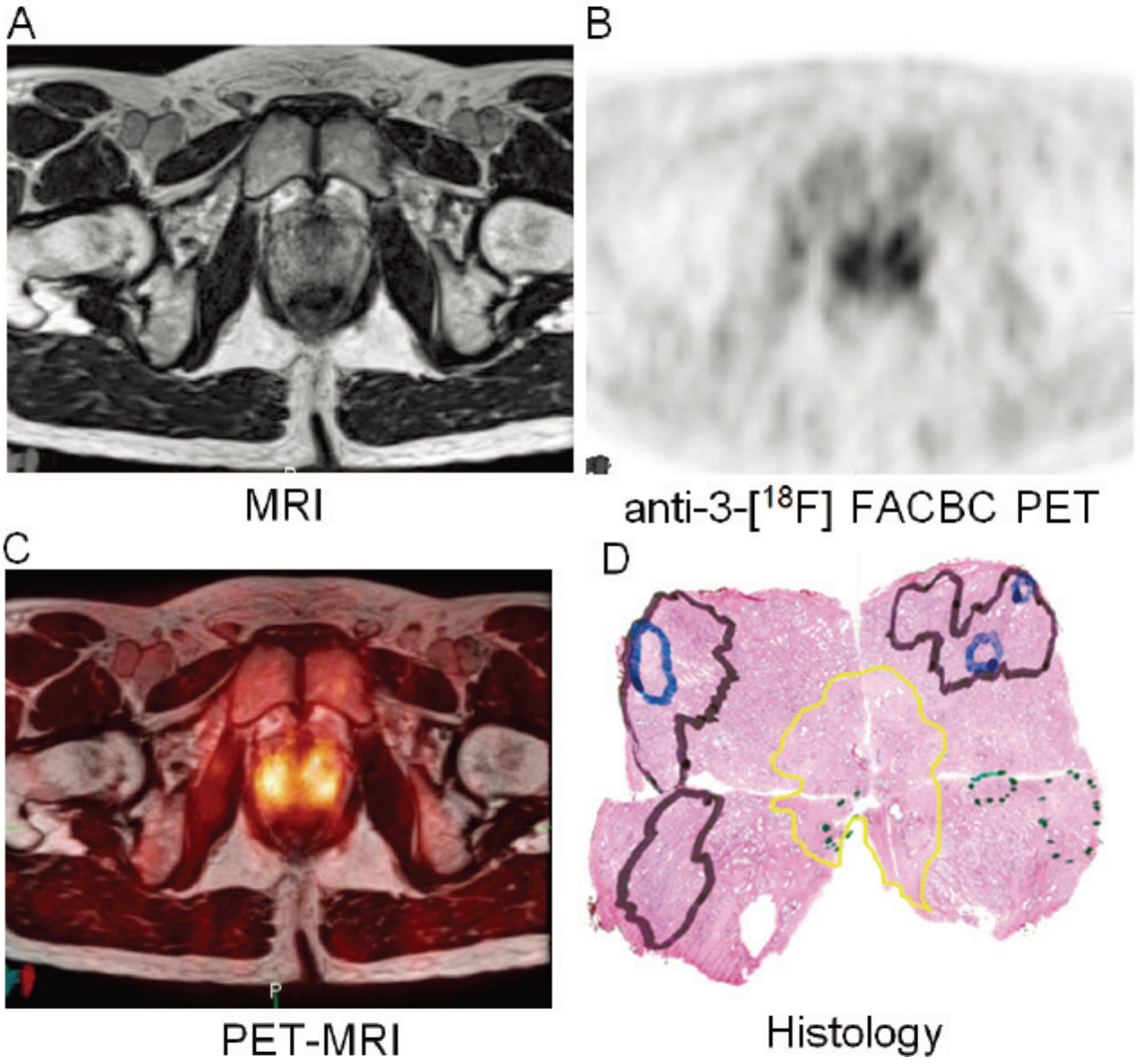

Figure 2. MR (A), *anti*-3-[^{18}F] FACBC PET acquired at 28 min post radiotracer administration (B), coregistered PET-MR (C) and histology (D).In this patient uptake in the right anterior and posterior and left anterior basal sextants correlate with presence of tumor but uptake in the left posterior sextant seems to correlate with inflammation. On the histology, solid black represent Gleason 3, solid blue represents Gleason 4, dotted green represents inflammation, and yellow represents BPH.

a correlation of Gleason score with SUVmax. However, overlap of uptake between malignant and non-malignant as well as Gleason categories would limit the utility of imaging in the place of histologic sampling.

Primary prostate carcinoma is the most frequently occurring cancer in men with over two hundred thousand cases diagnosed per year in the United States alone. In addition prostate cancer disproportionally strikes an older age group with an estimated median age of 79 at diagnosis [16]. Prostate cancer may also present as a spectrum from indolent disease to highly aggressive subtypes [2]. Because of the widespread use of PSA screening, prostate carcinoma is often detected at earlier stages when it may be curable, yet some variants do not require more than a watchful waiting approach, especially in older patients [17]. Due to the inherent sampling bias in routine sextant biopsy, disease may be over or underestimated [18]. Thus, an imaging technique which could more accurately describe extent and aggressiveness of tumor would be useful to direct therapy for individual patients. Current treatment decisions are typically based on nomograms. Imaging could also be potentially help-

Table 2A. Mean SUVmax for Malignant Versus Non-malignant Sextants

	4 min	16 min	28 min	40 min
Malignant SUVmax±SD (n=79)	5.1±2.6	4.5±1.6	4.0±1.3	3.8±1.0
Non-malignant SUVmax±SD (n=41)	4.0±1.9	3.5±0.8	3.4±0.9	3.3±0.9
p-value	0.0113	<.0001	0.0036	0.0069

Table 2B. Mean Total Sextant Activity (SUV*ml) for Malignant Versus Benign Sextants

	4 min	16 min	28 min	40 min
Malignant TSA±SD (n=79)	3.1±2	3.1±1.9	2.9±1.6	2.8±1.6
Non-malignant TSA±SD (n=41)	2.1±1.3	2.3±1.1	2.2±1.0	2.1±0.9
p-value	0.0007	0.0046	0.0099	0.0046

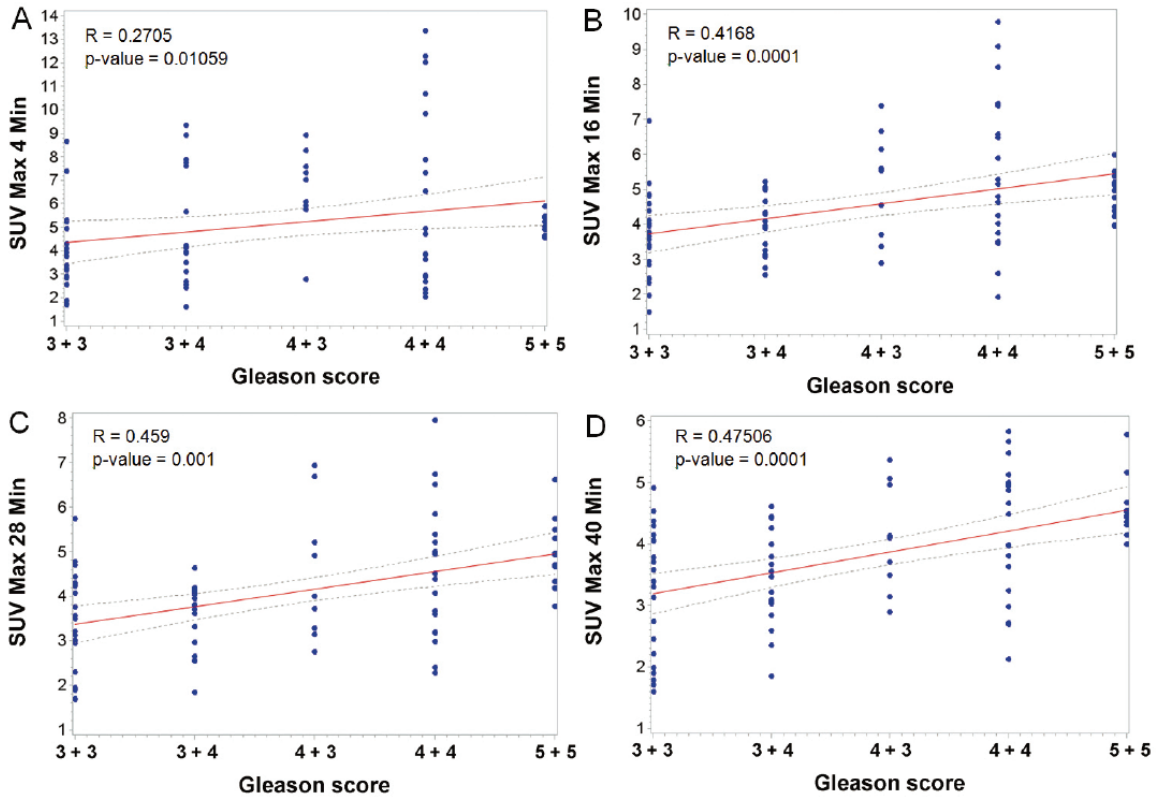

Figure 3. Correlation of *anti*-3-[^{18}F] FACBC SUV max at (A) 4 min, (B) 16 min, (C) 28min, and (D) 40 min with Gleason score.

ful in guiding biopsy to the most aggressive histologic subtype and to differentiate PSA elevation secondary to carcinoma versus PSA elevation from non-malignant entities such as BPH or prostatitis.

Amino acids are considered essential nutrients for multiplying tumor cells. A number of naturally and non-naturally occurring PET amino acid based radiotracers have been produced for the evaluation of prostate cancer [3, 19-21]. One of the first such radiotracers to be studied was the naturally occurring amino acid radiotracer, L-[^{11}C]methionine ([^{11}C]MET). In a study of 20 patients with elevated PSA levels and negative prostate biopsies, Toth and coworkers reported that, [^{11}C]MET was useful in directing subsequent biopsy in 7/15 patients with true positive uptake, but that 8/15 patients had high uptake and negative repeat biopsies show-

Table 3. Mean SUVmax of Low versus High Gleason Groups

	4mins	16mins	28mins	40mins
Low Gleason Group (n=38) SUVmax±SD	4.4±2.1	3.8±1.1	3.5±1.0	3.3±0.9
High Gleason Group (n=41) SUVmax±SD	5.9±2.8	5.2±1.7	4.7±1.3	4.3±0.9
p-value	0.0092	<0.0001	<0.0001	<0.0001

Low Gleason: GI 3+3 and 3+4; High Gleason: GI 4+3,4+4, 5+5.

ing BPH or chronic prostatitis [19]. All 5 patients with negative [^{11}C]MET PET had negative repeat biopsies. The findings with [^{11}C]MET PET of high sensitivity (100%), but low specificity (38%) is similar to the findings in the current study of sensitivity of 81.25% with a specificity of 50%. Direct comparisons are challenging though because of differences in methodology. Step section histologic analysis was conducted in the current study as compared to the biopsy approach of the [^{11}C]MET PET study.

Other PET radiotracers with different uptake mechanisms have also been studied in the evaluation of primary prostate carcinoma. These include ^{18}F-FDG, ^{11}C-Actetate, ^{11}C-Choline, and ^{18}F-Choline (FCH). ^{18}F-FDG detects carcinoma on the basis of increased glucose utilization of tumors with upregulated GLUT (glucose transporter expression) and hexokinase activity. Yet, similarity in FDG uptake between non-malignant and malignant prostate tissue has also been reported [22, 23]. In addition, excretion of FDG into the urinary system may limit evaluation of the pelvis due to intensity in the bladder.

The choline based radiotracers are taken up in prostate carcinoma via elevated presence of choline kinase found in malignant tissue. FCH as compared with ^{11}C-Choline demonstrates greater excretion into the urinary system. While some investigators have demonstrated significantly lower uptake in non-malignant versus malignant tissue, others have reported overlap in uptake between non-malignant and malignant tissue [5, 24-26].

Finally, ^{11}C-Actetate is believed to be taken up in prostate carcinoma due to the dominance of fatty acid metabolism in this tumor. Numerous investigators have also noted an overlap between uptake in malignant and non-malignant prostatic tissue [6, 27]. In a recent study by Mena and coworkers in which multiparametric MR was compared with ^{11}C-Actetate PET-CT in primary prostate carcinoma with gold standard established via whole mount step section histopathology and sophisticated modeling between histology and imaging, ^{11}C-Actetate demonstrated a sensitivity and specificity of 61.6 and 80.0% respectively, while similar values for multiparametric MR were 82.3% and 95.1%. In that study, ^{11}C-Actetate uptake neither correlated with Gleason score nor PSA values.

The mechanism of *anti*-3-[^{18}F] FACBC uptake has yet to be fully defined but has been reported to be primarily dependent upon sodium-dependent (ASC) and sodium-independent (L type) amino acid transport, specifically ASCT2 and LAT1 [10, 12]. Both ASCT2 and LAT1 have been implicated as important amino acid transporters with increased expression in many cancers [28]. LAT1 and ASCT2 have been associated with more aggressive biologic behavior in prostate carcinoma [29, 30]. It is interesting to note that in the current study there was a positive correlation of Gleason score and *anti*-3-[^{18}F] FACBC uptake with a step off in uptake between Gleason 3+4 and less and 4+3 and greater, a boundary which has been associated with more aggressive disease [31, 32]. Increased expression of both ASCT2 and LAT1 as expressed by increasing *anti*-3-[^{18}F] FACBC uptake may be an explanation of this phenomenon but more studies would have to be done to determine the definitive mechanism and practical utility.

Though we found a statistically significant difference between SUVmax and TSA between non-malignant and malignant sextants, and a good sensitivity by visual analysis, there was suboptimal specificity as well as a significant overlap of radiotracer activity between non-malignant and malignant sextants. Accuracy peaked at 28 minutes after injection by visual analysis, probably reflecting the most optimal balance between nonspecific background uptake as well as conspicuity of uptake in the

target lesion. LAT1, LAT2, and system ASC effect amino acid transport through a 1:1 exchange [10, 33]. Since one amino acid is transported out of the cell for every one that is transported into the cell, it is likely that this is the cause of decreasing *anti*-3-[^{18}F] FACBC activity with time within tumors. Specificity did not improve even after performing sub-analysis of tumor to background prostate ratios, retention indices, or comparison to other background structures (data not shown). Suboptimal specificity in the prostate bed with *anti*-3-[^{18}F] FACBC PET has also been reported by our group in post-therapy prostate cancer patients with suspicion of recurrence [8]. Turkbey also reported overlap of uptake profiles of this radiotracer with nonmalignant histology [34]. More research will be required to fully elucidate these findings.

We did not find a significant correlation of Ki-67 with SUVmax. Other immunohistochemical markers that we evaluated such as synaptophysin, P504s, chromogranin A, P53, androgen receptor, and prostein also did not correlate with *anti*-3-[^{18}F] FACBC uptake. While earlier investigation had demonstrated a positive non-significant trend, this did not bear out on more rigorous analysis [35]. Similarly, we have also found absence of correlation of *anti*-3-[^{18}F] FACBC uptake with Ki-67 in a study of malignant pulmonary nodules (Now, accepted in press, unpublished). Interestingly, mixed results have been reported in the literature as to histologic correlation of Ki-67 and Gleason score [36]. In addition, choline uptake has also not generally correlated with Ki-67 [5, 37].

A major limitation of our study is lack of step section whole mount histology at our institution which precluded utilizing sophisticated modeling to ensure an exact correlation of histology to imaging. Because of these limitations, we chose to analyze the data on a per sextant basis as to presence or absence of tumor only, since this would result in the least uncertainty as to imaging-histologic correlation given our resources. We therefore believed we could not accurately correlate imaging findings to individual sub-sextant regions of normal histology, BPH, tumor, PIN, or inflammation and that there is resultant intermixing of malignant and non-malignant signal in each sextant. Even so, we believe the questions raised by our findings could serve as a template for future investigation. We would recommend that this type of study only be undertaken at a center with whole mount histologic processing techniques and modeling [6].

In conclusion, in the evaluation of primary prostate carcinoma with *anti*-3-[^{18}F] FACBC PET, highest accuracy upon visual analysis is present at 28 minutes at which time there is sensitivity of 81.3%, specificity of 50.0%, with a positive predictive and negative predictive value of 76.5% and 57.1%, respectively. While there was a statistically significant difference between mean SUV max and total sextant activity between non-malignant and malignant sextants, overlap of radiotracer activity between non-malignant and malignant sextants would limit practical utility for such interventions as radiotherapy planning. Yet, the correlation between both higher Gleason scores and *anti*-3-[^{18}F] FACBC SUVmax could be useful to direct biopsy to areas of most aggressive disease. More study is required utilizing step section whole mount histology coupled with sophisticated co-registered modeling between histologic sections and imaging.

Acknowledgment

This is work is supported by the National Institutes of Health (P 50 CA 128301), with additional support from the Georgia Cancer Coalition. We also acknowledge the hard work Delicia Votaw, CNMT, Fenton G. Ingram, RT(R), CNMT, PET, Seraphinah Lawal, RT(R), CNMT, PET, Adam Brown, RT(N), CNMT, Ronald J. Crowe, RPh, BCNP, and the entire cyclotron and synthesis team, Leah-Madge Bellamy, RN, MSN, Beverly Hunter, RN, Michelle Faurot, BS, Ruth P. Westby, BA, James R. Galt, PhD, and John R. Votaw, PhD. We also gratefully acknowledge the contributions of Eric Jablonowski, AA, for media support.

Conflict of interest statement

Dr. Mark Goodman and Emory University are eligible to receive royalties from the licensing of *anti*-3-[^{18}F] FACBC.

Address correspondence to: Dr. David M Schuster, Division of Nuclear Medicine and Molecular Imaging, Department of Radiology and Imaging Sciences, Emory University Hospital, Room E152, 1364 Clifton Road, Atlanta, GA 30322, USA. Phone: 404-

7124859; Fax: 404-7124860; E-mail: dschust@emory.edu

References

[1] Siegel R, Naishadham D and Jemal A. Cancer statistics, 2012. CA Cancer J Clin 2012; 62: 10-29.

[2] Jadvar H and Alavi A. Role of Imaging in Prostate Cancer. PET Clin 2009; 4: 135-138.

[3] Schoder H and Larson SM. Positron emission tomography for prostate, bladder, and renal cancer. Semin Nucl Med 2004; 34: 274-292.

[4] Brawer MK, Ploch NR and Bigler SA. Prostate cancer tumor location as predicted by digital rectal examination transferred to ultrasound and ultrasound-guided prostate needle biopsy. J Cell Biochem Suppl 1992; 16H: 74-77.

[5] Jadvar H. Prostate cancer: PET with ^{18}F-FDG, ^{18}F- or ^{11}C-acetate, and ^{18}F- or ^{11}C-choline. J Nucl Med 2011; 52: 81-89.

[6] Mena E, Turkbey B, Mani H, Adler S, Valera VA, Bernardo M, Shah V, Pohida T, McKinney Y, Kwarteng G, Daar D, Lindenberg ML, Eclarinal P, Wade R, Linehan WM, Merino MJ, Pinto PA, Choyke PL and Kurdziel KA. ^{11}C-Acetate PET/CT in localized prostate cancer: a study with MRI and histopathologic correlation. J Nucl Med 2012; 53: 538-545.

[7] Jani AB, Fox TH, Whitaker D and Schuster DM. Case study of anti-1-amino-3-F-18 fluorocyclobutane-1-carboxylic acid (anti-[F-18] FACBC) to guide prostate cancer radiotherapy target design. Clin Nucl Med 2009; 34: 279-284.

[8] Schuster DM, Savir-Baruch B, Nieh PT, Master VA, Halkar RK, Rossi PJ, Lewis MM, Nye JA, Yu W, Bowman FD and Goodman MM. Detection of Recurrent Prostate Carcinoma with anti-1-Amino-3-^{18}F-Fluorocyclobutane-1-Carboxylic Acid PET/CT and ^{111}In-Capromab Pendetide SPECT/CT. Radiology 2011; 259: 852-861.

[9] Schuster DM, Votaw JR, Nieh PT, Yu W, Nye JA, Master V, Bowman FD, Issa MM and Goodman MM. Initial Experience with the Radiotracer Anti-1-Amino-3-^{18}F-Fluorocyclobutane-1-Carboxylic Acid with PET/CT in Prostate Carcinoma. J Nucl Med 2007; 48: 56-63.

[10] Oka S, Okudaira H, Yoshida Y, Schuster DM, Goodman MM and Shirakami Y. Transport mechanisms of trans-1-amino-3-fluoro[1-(14)C]cyclobutanecarboxylic acid in prostate cancer cells. Nucl Med Biol 2012; 39: 109-119.

[11] Oka S, Hattori R, Kurosaki F, Toyama M, Williams LA, Yu W, Votaw JR, Yoshida Y, Goodman MM and Ito O. A Preliminary Study of Anti-1-Amino-3-^{18}F-Fluorocyclobutyl-1-Carboxylic Acid for the Detection of Prostate Cancer. J Nucl Med 2007; 48: 46-55.

[12] Okudaira H, Shikano N, Nishii R, Miyagi T, Yoshimoto M, Kobayashi M, Ohe K, Nakanishi T, Tamai I, Namiki M and Kawai K. Putative Transport Mechanism and Intracellular Fate of Trans-1-Amino-3-^{18}F-Fluorocyclobutanecarboxylic Acid in Human Prostate Cancer. J Nucl Med 2011; 52: 822-829.

[13] McConathy J, Voll RJ, Yu W, Crowe RJ and Goodman MM. Improved synthesis of anti-[^{18}F] FACBC: improved preparation of labeling precursor and automated radiosynthesis. Appl Radiat Isot 2003; 58: 657-666.

[14] Mattes D, Haynor DR, Vesselle H, Lewellen TK and Eubank W. PET-CT image registration in the chest using free-form deformations. IEEE Trans Med Imaging 2003; 22: 120-128.

[15] Yamaguchi T, Lee J, Uemura H, Sasaki T, Takahashi N, Oka T, Shizukuishi K, Endou H, Kubota Y and Inoue T. Prostate cancer: a comparative study of ^{11}C-choline PET and MR imaging combined with proton MR spectroscopy. Eur J Nucl Med Mol Imaging 2005; 32: 742-748.

[16] Yancik R. Population aging and cancer: a cross-national concern. Cancer J 2005; 11: 437-441.

[17] NCCN Clinical Practice Guidelines in Oncology: Prostate Cancer. Version 1.2013. Available at: http://www.nccn.org/professionals/physician_gls/pdf/prostate.pdf. Accessed Dec 10 2012.

[18] Corcoran NM, Hovens CM, Hong MK, Pedersen J, Casey RG, Connolly S, Peters J, Harewood L, Gleave ME, Goldenberg SL and Costello AJ. Underestimation of Gleason score at prostate biopsy reflects sampling error in lower volume tumours. BJU Int 2012; 109: 660-664.

[19] Toth G, Lengyel Z, Balkay L, Salah MA, Tron L and Toth C. Detection of prostate cancer with ^{11}C-methionine positron emission tomography. J Urol 2005; 173: 66-69; discussion 69.

[20] Kalkner KM, Ginman C, Nilsson S, Bergstrom M, Antoni G, Ahlstrom H, Langstrom B and Westlin JE. Positron emission tomography (PET) with ^{11}C-5-hydroxytryptophan (5-HTP) in patients with metastatic hormone-refractory prostatic adenocarcinoma. Nucl Med Biol 1997; 24: 319-325.

[21] Hong H, Zhang Y, Sun J and Cai W. Positron emission tomography imaging of prostate cancer. Amino Acids 2010; 39: 11-27.

[22] Salminen E, Hogg A, Binns D, Frydenberg M and Hicks R. Investigations with FDG-PET scanning in prostate cancer show limited value for clinical practice. Acta Oncol 2002; 41: 425-429.

[23] Kao PF, Chou YH and Lai CW. Diffuse FDG uptake in acute prostatitis. Clin Nucl Med 2008; 33: 308-310.

[24] Farsad M, Schiavina R, Castellucci P, Nanni C, Corti B, Martorana G, Canini R, Grigioni W, Boschi S, Marengo M, Pettinato C, Salizzoni E, Monetti N, Franchi R and Fanti S. Detection and localization of prostate cancer: correlation of (^{11})C-choline PET/CT with histopathologic step-section analysis. J Nucl Med 2005; 46: 1642-1649.

[25] Igerc I, Kohlfurst S, Gallowitsch HJ, Matschnig S, Kresnik E, Gomez-Segovia I and Lind P. The value of ^{18}F-choline PET/CT in patients with elevated PSA-level and negative prostate needle biopsy for localisation of prostate cancer. Eur J Nucl Med Mol Imaging 2008; 35: 976-983.

[26] Reske SN, Blumstein NM, Neumaier B, Gottfried HW, Finsterbusch F, Kocot D, Moller P, Glatting G and Perner S. Imaging prostate cancer with ^{11}C-choline PET/CT. J Nucl Med 2006; 47: 1249-1254.

[27] Kato T, Tsukamoto E, Kuge Y, Takei T, Shiga T, Shinohara N, Katoh C, Nakada K and Tamaki N. Accumulation of [^{11}C]acetate in normal prostate and benign prostatic hyperplasia: comparison with prostate cancer. Eur J Nucl Med Mol Imaging 2002; 29: 1492-1495.

[28] Fuchs BC and Bode BP. Amino acid transporters ASCT2 and LAT1 in cancer: partners in crime? Semin Cancer Biol 2005; 15: 254-266.

[29] Sakata T, Ferdous G, Tsuruta T, Satoh T, Baba S, Muto T, Ueno A, Kanai Y, Endou H and Okayasu I. L-type amino-acid transporter 1 as a novel biomarker for high-grade malignancy in prostate cancer. Pathol Int 2009; 59: 7-18.

[30] Li R, Younes M, Frolov A, Wheeler TM, Scardino P, Ohori M and Ayala G. Expression of neutral amino acid transporter ASCT2 in human prostate. Anticancer Res 2003; 23: 3413-3418.

[31] Chan TY, Partin AW, Walsh PC and Epstein JI. Prognostic significance of Gleason score 3+4 versus Gleason score 4+3 tumor at radical prostatectomy. Urology 2000; 56: 823-827.

[32] Wright JL, Salinas CA, Lin DW, Kolb S, Koopmeiners J, Feng Z and Stanford JL. Prostate cancer specific mortality and Gleason 7 disease differences in prostate cancer outcomes between cases with Gleason 4 + 3 and Gleason 3 + 4 tumors in a population based cohort. J Urol 2009; 182: 2702-2707.

[33] McConathy J, Yu W, Jarkas N, Seo W, Schuster DM and Goodman MM. Radiohalogenated nonnatural amino acids as PET and SPECT tumor imaging agents. Med Res Rev 2012; 32: 868-905.

[34] Turkbey B, Mena E, Adler S, Lax M, Bernado M, Withers B, Pinto P, Merino M, Kurdziel K and Choyke P. GE-148 (^{18}F) injection PET/CT imaging and multiparametric MRI for detection of localized prostate cancer using customized MRI-based specimen molds. J Nucl Med 2011; 52: 1906.

[35] Taleghani P, Amzat R, Osunkoya A, Savir-Baruch B, Nieh P, Master V, Fei B, Fox T, Goodman M and Schuster D. Increased expression of Ki-67 correlates with synthetic amino acid PET radiotracer uptake in prostate cancer. J Nucl Med 2012; 53: 1097.

[36] Revelos K, Petraki C, Gregorakis A, Scorilas A, Papanastasiou P, Tenta R and Koutsilieris M. p27(kip1) and Ki-67 (MIB1) immunohistochemical expression in radical prostatectomy specimens of patients with clinically localized prostate cancer. In vivo 2005; 19: 911-920.

[37] Breeuwsma AJ, Pruim J, Jongen MM, Suurmeijer AJ, Vaalburg W, Nijman RJ and de Jong IJ. In vivo uptake of [^{11}C]choline does not correlate with cell proliferation in human prostate cancer. Eur J Nucl Med Mol Imaging 2005; 32: 668-673.

Schuster DM, Taleghani PA, Nieh PT, Master VA, Amzat R, Savir-Baruch B, Halkar RK, Fox T, Osunkoya AO, Nye JA, Yu W, Fei BW, Wang Z, Chen Z, Goodman MM, Characterization of primary prostate carcinoma by anti-1-amino-2-[18F] -fluorocyclobutane-1-carboxylic acid (anti-3-[18F] FACBC) uptake, American Journal of Nuclear Medicine and Molecular Imaging 2013; 3(1):85-96.

AJNMMI Copyright© 2013. One print or electronic copy may be made for personal use only. Systematic reproduction and distribution, duplication of any material in this paper for a fee or for commercial purposes, or modification of the content of the paper are prohibited.